LETTERS

Efficacy of the post-perovskite phase as an explanation for lowermost-mantle seismic properties

James Wookey[1]†, Stephen Stackhouse[2], J-Michael Kendall[3], John Brodholt[2] & G. David Price[2]

Constraining the chemical, rheological and electromagnetic properties of the lowermost mantle (D″) is important to understand the formation and dynamics of the Earth's mantle and core. To explain the origin of the variety of characteristics of this layer observed with seismology, a number of theories have been proposed[1], including core–mantle interaction, the presence of remnants of subducted material and that D″ is the site of a mineral phase transformation. This final possibility has been rejuvenated by recent evidence for a phase change in $MgSiO_3$ perovskite (thought to be the most prevalent phase in the lower mantle[2]) at near core–mantle boundary temperature and pressure conditions[3]. Here we explore the efficacy of this 'post-perovskite' phase to explain the seismic properties of the lowermost mantle through coupled *ab initio* and seismic modelling of perovskite and post-perovskite polymorphs of $MgSiO_3$, performed at lowermost-mantle temperatures and pressures. We show that a post-perovskite model can explain the topography and location of the D″ discontinuity, apparent differences in compressional- and shear-wave models[1] and the observation of a deeper, weaker discontinuity[4,5]. Furthermore, our calculations show that the regional variations in lower-mantle shear-wave anisotropy are consistent with the proposed phase change in $MgSiO_3$ perovskite.

The elastic and seismic properties of mineral crystals can be determined using *ab initio* methods, which solve (to a good approximation) Schrödinger's equation to model interactions in a system of nuclei and electrons. Of these, density functional theory[6] (DFT) is one of the most reliable and efficient methods. DFT-based methods explicitly incorporating thermal effects have been applied to the perovskite and post-perovskite polymorphs of $MgSiO_3$ at lower-mantle pressures but primarily at low temperatures[7–9]. Here we apply the technique of ref. 10 to $MgSiO_3$ at temperatures and pressures appropriate for the D″ region (see Fig. 1; see also the Supplementary Information for details of method, results and comparison with previous work[8,9,11]). This provides us with the opportunity to assess directly the efficacy of a post-perovskite phase in explaining the seismic observations.

A sharp discontinuity in seismic velocity is observed in many places in the lowermost mantle (for a review see ref. 1). The depth of this feature varies considerably (150–450 km above the core–mantle boundary, CMB). On the basis of low-temperature analyses, it has been suggested that the transformation to a post-perovskite structure in $MgSiO_3$ is responsible for the observed seismic discontinuity[7,9,12], though this has been hitherto difficult to quantify and compare with the effects of pure thermal variation. Our *ab initio* simulations, however, give us the opportunity to do this: we can interpolate the five calculated sets of elastic parameters for each phase over a realistic temperature and pressure regime for the lowermost mantle. We take three depth–temperature profiles from a mantle convection model[4] (representing a hot, cold and average part of the lower mantle, see Fig. 1). We then convert the temperature profiles to velocity and density profiles, both with and without a transformation to post-perovskite (Fig. 2). The Clapeyron slope for the phase transformation has been calculated as 7.5 MPa K^{-1} (ref. 12), and 9.56 MPa K^{-1} (ref. 7). We use the latter value and a static transition pressure of 98.7 GPa (ref. 7).

The depth of the phase transition is strongly temperature-dependent, to the extent that it never occurs for the hot-region profile. This could explain the topography observed on the D″ discontinuity and the difficulty of confidently observing it in the regions of the lowermost mantle characterized by low seismic

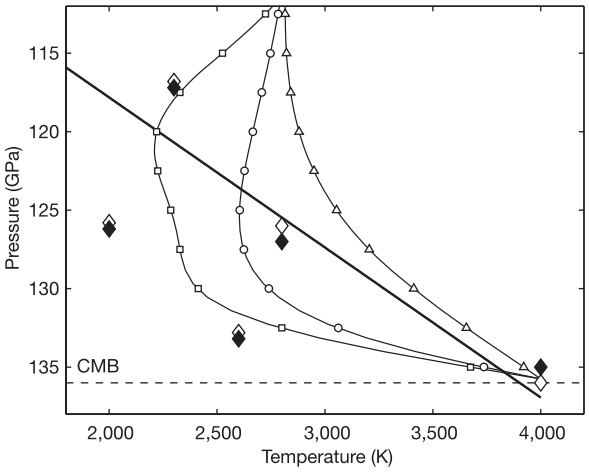

Figure 1 | Phase boundary[7] and calculation points for the perovskite and post-perovskite polymorphs of $MgSiO_3$. We show the variation of temperature with pressure for three vertical profiles in a mantle convection model[4]. These come from 'hot' (triangles), 'cold' (squares) and 'average' (circles) parts of the mantle. Also plotted is the phase boundary from ref. 7; $MgSiO_3$ has a perovskite structure above this line, and a post-perovskite form below it. The 'cold' and 'average' profiles cross this boundary twice, thus predicting a thick post-perovskite layer underlain by a thin perovskite layer (similar to ref. 5). The 'hot' profile does not cross the phase boundary at all. It should be noted that this linear phase boundary is approximate; deviation from this will change the transition pressure. The dashed line indicates the CMB. The open and solid diamonds show the positions for which we have *ab initio* calculations of the seismic properties of the perovskite and post-perovskite, respectively.

[1]School of Earth and Environment, University of Leeds, Leeds LS2 9JT, UK. [2]Department of Earth Sciences, University College London, Gower Street, London WC1E 6BT, UK. [3]Department of Earth Sciences, University of Bristol, Wills Memorial Building, Queens Road, Bristol BS8 1RJ, UK. †Present address: Department of Earth Sciences, University of Bristol, Wills Memorial Building, Queens Road, Bristol BS8 1RJ, UK.

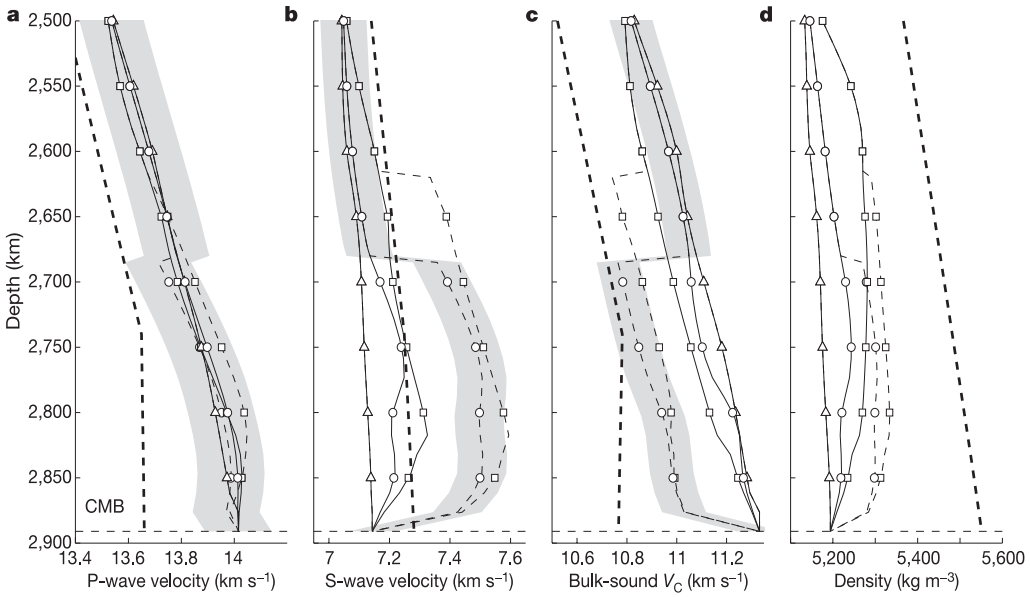

Figure 2 | Seismic properties interpolated from *ab initio* calculations. These show the P-wave (**a**) and S-wave (**b**) velocities, the bulk-sound speed (**c**) and the density (**d**) for the 'hot' (triangles), 'average' (circles) and 'cold' (squares) mantle convection profiles. These are converted from the temperature profiles in Fig. 1 into variation of the seismic properties with depth by interpolation of our *ab initio* results. The solid traces are the variation solely due to temperature (in perovskite), and the dashed lines are where a phase-transformation is included. The shaded area shows the estimated constraint for the average profile (other profiles are similarly constrained). For comparison the velocities and density from the reference model ak135 (ref. 15) are included (black dashed trace).

velocities (such as the central Pacific)[1]. The phase transition has different effects on the seismic velocities. The S-wave velocity (V_S) increases by around 4% at the discontinuity; this is enough to produce a strong shear-wave reflection. In contrast, the bulk-sound speed (V_C) is as strongly reduced; this anticorrelation results in almost no P-wave velocity discontinuity. This is similar to previous athermal results[7,9,11]. It is interesting to note that the strongest effect is in the 'average' profile, implying that it is not confined to the coldest

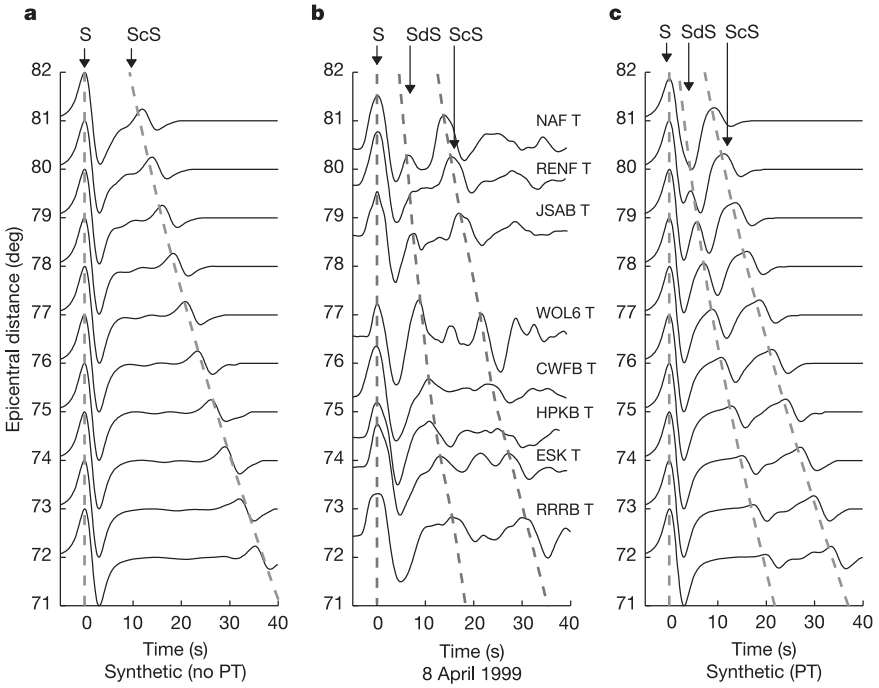

Figure 3 | Comparison between real and synthetic S-wave seismograms predicted from the velocity/density profiles shown in Fig. 2. **b**, Data from an earthquake on 8 April 1999 recorded at temporary stations (names as shown) in the SPICED array[30] and permanent stations in France and the UK. **a**, **c**, Synthetics generated using reflectivity modelling[17]: **a** shows the results of a purely thermal model; **c** includes the effects of a phase change. The upper and lower discontinuity depths are constrained to be those observed for this event (approximately 250 km and 60 km above the CMB respectively[4]). Grey dashed lines show the travel times of the direct, D″-reflected and core-reflected phases calculated using ray tracing. A D″ reflection is observed in the phase-change model that is very similar in character to the one observed for the data. This is absent from the thermal model. PT, phase transformation.

parts of the lowermost mantle. Furthermore, our results show that an anticorrelation of V_C and V_S in the lower mantle as seen in some tomography models[13,14] might be explained by a phase change in $MgSiO_3$. (The velocity anomalies in these models are relative to a global average at each depth, so warmer, perovskite-rich regions would appear fast in V_C and slow in V_S relative to the average, and vice versa for cooler, post-perovskite-rich regions).

The temperature–pressure curves for both 'cold' and 'average' mantle cross the phase boundary twice, providing a possible explanation for the second, deeper discontinuity which has been observed in the lowermost mantle[4,5]. We predict this to occur at around 20 km above the CMB, whereas seismic observations suggest 60–80 km. This is, however, very sensitive to both the slope and intercept of the phase boundary and the temperature at the CMB (which is only known to within a few hundred Kelvin). We have also assumed a linear phase boundary, which may not be accurate. If the two observed discontinuities are related to this phase change, the topography on them should be anticorrelated; however, ascertaining whether this is the case requires more seismic observations.

The density profile shows a significant deviation from the average value given by the reference model ak135 (ref. 15). This is probably due to a combination of factors, but the most significant may be the absence of iron in the *ab initio* calculations. Incorporation of 15 mole per cent $FeSiO_3$ is sufficient to account for the density discrepancy, though also including less-dense[16] MgO may increase this slightly (~1–2%). Differences between ak135 and the predicted seismic velocities are less than the estimated errors combined with the expected constraint in a one-dimensional reference model.

We apply reflectivity modelling[17] to generate synthetic S-wave seismic sections (Fig. 3). With a phase-change model, an SdS reflection very similar to that observed in real data are evident. In P-wave synthetics no strong PdP phase is observed for either the thermal or phase-change model (see Supplementary Fig. S3). This is due to the anticorrelation of the bulk and shear moduli, which both contribute to P-wave velocity. However, the amplitude of this phase can be considerably enhanced by anisotropy in the lowermost mantle (see Supplementary Information and Supplementary Fig. S4), so observations of PdP could be consistent with a phase change model in regions of strong deformation. Our synthetics represent the seismic effect associated solely with the presence of a phase transformation, and they show that such a phenomenon effectively produces realistic seismic reflections.

The lowermost mantle also has a strong anisotropic signature. Seismic anisotropy (the variation of velocity with direction of wave propagation) provides a signature of deformation processes in the Earth. For example, measurements of anisotropy in the upper mantle have been used to study the dynamics of past and contemporary tectonics (see review in, for example, ref. 18). The anisotropy of the lowermost mantle has also been studied extensively (see reviews in refs 18 and 19). These studies have mainly restricted themselves to looking for radial anisotropy (also called vertical transverse isotropy, VTI), that is, measuring the difference in travel time between the horizontally (SH) and vertically polarized (SV) components of shear body-wave phases such as S, S_{diff} and ScS. In a recent study, a large data set of body-wave and surface-wave phases were inverted for shear-wave velocity and radial anisotropy, providing long-wavelength coverage of the whole mantle[20]. This model shows a general trend of SH phases arriving before SV (that is, a horizontally polarized fast shear wave) in the faster regions of the lowermost mantle (which is inferred to be colder). This is also seen in globally averaged models[21]. This anisotropy is much smaller in the slower (and thus hotter) regions, such as the central Pacific, and does not show a consistent trend of fast-shear-wave orientation[19,20].

Several mechanisms have been suggested to explain observations of lowermost-mantle anisotropy. Perhaps the most obvious explanation is the lattice-preferred orientation (LPO) of the phases thought to comprise the bulk of the lower mantle: $MgSiO_3$ and MgO (ref. 2). This requires a favourable deformation regime (dislocation creep as opposed to diffusion creep) to form an aggregate anisotropic medium. This has been observed experimentally at uppermost lower-mantle conditions[22] for $MgSiO_3$. However, the LPO of perovskite $MgSiO_3$ has not been thought to be a viable candidate mechanism, as it does not produce a horizontal fast-shear wave[8,18]. The LPO of MgO (ref. 16) is more plausible, but it is a much less abundant phase. Another suggested mechanism is the shape-preferred orientation (SPO) of inclusions of a secondary phase. If this phase has strongly contrasting elastic properties to those of the matrix (for example, if the inclusion were remnant basaltic melt[23]), then strong shear-wave anisotropy might result[18].

The presence of post-perovskite $MgSiO_3$ provides a perhaps simpler explanation. The observed lateral variability of anisotropy in the lowermost mantle might be explained by thermal or compositional effects (or a combination of both). The *ab initio* calculations we have described provide the full elastic tensor for the perovskite and post-perovskite polymorphs of $MgSi0_3$. These indicate that perovskite with a glide plane normal to the [001] axis[22] shows a vertically polarized fast shear-wave. The slip systems of post-perovskite are unknown; however, with an glide plane normal to [001] post-perovskite shows a horizontally polarized fast shear-wave for all azimuths (Fig. 4), as is observed for the cold regions of the lowermost mantle[20]. This analysis suggests that post-perovskite provides a good explanation for the anisotropy observed in the cold regions of the lowermost mantle. At the present time, it does not conflict with any of the observational or laboratory evidence. This does not imply that other mechanisms of anisotropy may not contribute, but they are not required by current observations.

The analyses we have presented show that a phase transition in $MgSiO_3$ is a compelling explanation for many of the seismic properties observed for the lowermost mantle. The sharp velocity change required to observe a reflected P and S phase is much easier to produce with a phase change than purely by thermal variation. The anisotropy observed in the cold part of the lowermost mantle can also be explained in this manner. The horizontal fast-shear wave we

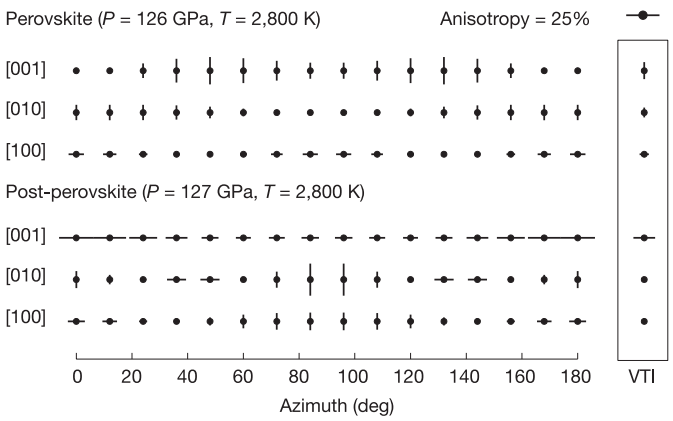

Figure 4 | Fast shear-wave orientation predicted for single-crystal perovskite and post-perovskite polymorphs of $MgSiO_3$ as a function of azimuth. The ray paths of the phases generally used to observe lowermost-mantle anisotropy[19] (S, ScS, S_{diff}) are very close to horizontal at the base of the mantle. Each black vector indicates the orientation of the fast shear-wave for a given (horizontal) propagation direction, scaled by anisotropy magnitude. The lowermost mantle seems to be predominantly transversely isotropic, with a horizontally polarized fast shear wave[19–21] (that is, $V_{SH} > V_{SV}$). For perovskite with a [001] glide plane (as is observed for the top of the lower mantle[22]), a vertical fast shear-wave is predicted. A horizontal fast shear-wave is predicted for post-perovskite with a [001] glide plane. Perovskite with a [100] glide plane also shows $V_{SH} > V_{SV}$, but the anisotropy is much smaller. This implies that post-perovskite at realistic conditions is a much better candidate for explaining lowermost-mantle anisotropy.

predict for post-perovskite is in agreement with observations, and the absence of the phase in the hotter regions may explain why no consistent trend is seen beneath the central Pacific[19]. The apparent anticorrelation between bulk-sound speed and shear-wave velocity anomalies reported for the lower mantle[13,14] can also be explained with a phase transformation, although this does not preclude a contribution of chemical origin. If present, chemical heterogeneity might also account for small-scale features such as basal ultralow-velocity zones[24] and scatterers[25,26].

We argue that post-perovskite $MgSiO_3$ is therefore likely to be both present and relatively abundant in the cold regions of the lowermost mantle, though we do not exclude the possibility of an additional source of chemical heterogeneity such as the presence of remnant slab material or core intrusion. The lowermost mantle is an important boundary to both mantle[27] and core convection[28], and the presence of this post-perovskite has implications for both. Convection in the core may be influenced by the mantle in several ways, and the thermal and electrical conductivity of D″ are an important and as-yet-unknown quantity. The presence of a dense basal layer may also significantly affect the style of convection in the mantle, controlling the timescale and morphology of features such as plumes[29].

Received 26 July; accepted 18 October 2005.

1. Wysession, M. E., *et al.* in *The Core-Mantle Boundary Region* (eds Gurnis, M., Wysession, M. E., Knittle, E. & Buffett, B. A.) Vol. 28, 273–297 (American Geophysical Union, Washington DC, 1998).
2. Ringwood, A. E. Phase transformations and their bearing on the constitution and dynamics of the mantle. *Geochim. Cosmochim. Acta* **55,** 2083–2110 (1991).
3. Murakami, M., Hirose, K., Kawamura, K., Sata, N. & Ohishi, Y. Post-perovskite phase transition in MgSiO3. *Science* **304,** 855–857 (2004).
4. Thomas, C., Kendall, J.-M. & Lowman, J. Lower-mantle seismic discontinuities and the thermal morphology of subducted slabs. *Earth Planet. Sci. Lett.* **225,** 105–113 (2004).
5. Herlund, J. W., Thomas, C. & Tackley, P. J. A doubling of the post-perovskite phase boundary and structure of the Earth's lowermost mantle. *Nature* **434,** 882–886 (2005).
6. Hohenberg, P. & Kohn, W. Inhomogeneous electron gas. *Phys. Rev. B* **136,** 864–871 (1964).
7. Oganov, A. R. & Ono, S. Theoretical and experimental evidence for a post-perovskite phase of $MgSiO_3$ in Earth's D″ layer. *Nature* **430,** 445–448 (2004).
8. Wentzcovitch, R. M., Karki, B. B., Karato, S. & Da Silva, C. R. S. High pressure elastic anisotropy of $MgSiO_3$ perovskite and geophysical implications. *Earth Planet. Sci. Lett.* **164,** 371–378 (1998).
9. Tsuchiya, T., Tsuchiya, J., Umemoto, K. & Wentzcovitch, R. M. Elasticity of post-perovskite $MgSiO_3$. *Geophys. Res. Lett.* **31,** L14603 (2004).
10. Stackhouse, S., Brodholt, J. P., Price, G. D., Wookey, J. & Kendall, J.-M. The effect of temperature on the acoustic anisotropy of the perovskite and post-perovskite polymorphs of MgSiO3. *Earth Planet. Sci. Lett.* **230,** 1–10 (2005).
11. Iitaka, T., Hirose, K., Kawamura, K. & Murakami, M. The elasticity of the $MgSiO_3$ post-perovskite phase in the Earth's lowermost mantle. *Nature* **430,** 442–445 (2004).
12. Tsuchiya, T., Tsuchiya, J., Umemoto, K. & Wentzcovitch, R. M. Phase transition in $MgSiO_3$ perovskite in the Earth's lower mantle. *Earth Planet. Sci. Lett.* **224,** 241–248 (2004).
13. Masters, G., Laske, G., Bolton, H. & Dziewonski, A. M. in *Earth's Deep Interior: Mineral physics and Tomography From the Atomic to the Global Scale* (eds Karato, S., Forte, A., Liebermann, R., Masters, G. & Stixrude, L.) Vol. 117, 201–213 (American Geophysical Union, Washington DC, 2000).
14. Trampert, J., Deschamps, F., Resovsky, J. & Yuen, D. Probabilistic tomography maps chemical heterogeneities throughout the lower mantle. *Science* **306,** 853–856 (2004).
15. Kennett, B. L. N., Engdahl, E. R. & Buland, R. Constraints on seismic velocities in the Earth from traveltimes. *Geophys. J. Int.* **122,** 108–124 (1995).
16. Karki, B. B., Wentzcovitch, R. M., Gironcoli, S. d. & Baroni, S. First-principles determination of elastic anisotropy and wave velocities of MgO at lower mantle conditions. *Science* **286,** 1705–1707 (1999).
17. Mueller, G. The reflectivity method; a tutorial. *Z. Geophys.* **58,** 153–174 (1985).
18. Kendall, J.-M. in *Earth's Deep Interior: Mineral physics and Tomography From the Atomic to the Global Scale* (eds Karato, S., Forte, A., Liebermann, R., Masters, G. & Stixrude, L.) Vol. 117, 133–159 (American Geophysical Union, Washington DC, 2000).
19. Lay, T., Williams, Q., Garnero, E. J., Kellogg, L. & Wysession, M. E. in *The Core-Mantle Boundary Region* (eds Gurnis, M., Wysession, M. E., Knittle, E. & Buffett, B. A.) Vol. 28, 299–318 (American Geophysical Union, Washington DC, 1998).
20. Panning, M. & Romanowicz, B. Inferences on flow at the base of Earth's mantle based on seismic anisotropy. *Science* **303,** 351–353 (2004).
21. Montagner, J.-P. & Kennett, B. L. N. How to reconcile body-wave and normal-mode reference Earth models. *Geophys. J. Int.* **125,** 229–248 (1996).
22. Cordier, P., Ungar, T., Zsoldos, L. & Tichy, G. Dislocation creep in $MgSiO_3$. *Nature* **428,** 837–840 (2004).
23. Hirose, K., Fei, Y., Ma, Y. & Mao, H.-K. The fate of subducted basaltic crust in the Earth's lower mantle. *Nature* **397,** 53–56 (1999).
24. Garnero, E. J., Revenaugh, J., Lay, T. & Kellog, L. H. in *The Core-Mantle Boundary Region* (eds Gurnis, M., Wysession, M. E., Knittle, E. & Buffett, B. A.) **Vol. 28** 319–334 (American Geophysical Union, Washington DC, 1998).
25. Thomas, C., Weber, M., Wicks, C. W. & Scherbaum, F. Small scatterers in the lower mantle observed at German broadband arrays. *J. Geophys. Res.* **104,** 15073–15088 (1999).
26. Brana, L. & Helffrich, G. A scattering region near the core-mantle boundary under the North Atlantic. *Geophys. J. Int.* **158,** 625–636 (2004).
27. Tackley, P. J. in *The Core-Mantle Boundary Region* (eds Gurnis, M., Wysession, M. E., Knittle, E. & Buffett, B. A.) Vol. 28, 231–253 (American Geophysical Union, Washington DC, 1998).
28. Gubbins, D. Geomagnetic polarity reversals: a connection with secular variation and core-mantle interaction? *Rev. Geophys.* **32,** 61–83 (1994).
29. Jellinek, A. M. & Manga, M. The influence of a chemical boundary layer on the fixity, spacing and lifetime of mantle plumes. *Nature* **418,** 760–763 (2002).
30. Kendall, J.-M. & Helffrich, G. SPICED: imaging the deep Earth. *Astron. Geophys.* **42,** 26–29 (2001).

Supplementary Information is linked to the online version of the paper at www.nature.com/nature.

Acknowledgements We thank D. Dobson for discussions. This work was supported by the Deep Earth System NERC consortium grant.

Author Information Reprints and permissions information is available at npg.nature.com/reprintsandpermissions. The authors declare no competing financial interests. Correspondence and requests for materials should be addressed to J.W. (j.wookey@bristol.ac.uk).